Modelling the physico-chemical speciation of plutonium in the eastern Irish Sea: a further development

R. Periáñez *

Departamento Física Aplicada I, Universidad de Sevilla, EU Ingeniería Técnica Agrícola, Ctra. Utrera km 1, E-41013 Seville, Spain

Abstract

A numerical full three-dimensional model previously developed to simulate the physico-chemical speciation of plutonium in the eastern Irish Sea has been improved. The model solves simultaneously the hydrodynamic equations, the suspended matter equation and the equations that give the time evolution of Pu concentrations in water, suspended matter and bottom sediments. It is considered that Pu may exist in each phase in two different oxidation states. Redox reactions are also considered. In the earlier version of the model, a one-step kinetic model was used to describe the transfers of radionuclides between the dissolved and solid phases. Although with this kind of model the contamination of the sediments can be properly simulated, it is clearly not able to describe the re-dissolution of radionuclides from a contaminated sediment once the external source to the sea is reduced. Thus, the model has been improved by substituting the one-step model with a two-step kinetic model consisting of two consecutive reversible reactions. Now it is possible to simulate both the sediment contamination and the re-dissolution processes.

Keywords: Plutonium; Irish Sea; Modelling; Sediments; Kinetic coefficients; Speciation

* Tel.: +34-954-486474; fax: +34-954-232644.
E-mail address: rperianez@us.es (R. Periáñez).

1. Introduction

Over the past few years, models for simulating the dispersion of non-conservative radionuclides in the marine environment have been developed in terms of kinetic transfer coefficients (Aldridge, 1998; Margvelashvily, Maderich, & Zheleznyak, 1997; Periáñez, 2000a, 2000b; Periáñez, Abril, & García-León, 1996; Piasecki, 1998), instead of the less appropriate equilibrium distribution coefficient, k_d. A one-step reversible model for the exchanges of radionuclides between the dissolved and solid (suspended matter and bottom sediments) phases is applied in all of the above-mentioned references:

$$R + XS \underset{k_2}{\overset{k_1}{\rightleftharpoons}} RS + X, \tag{1}$$

where R is the dissolved radionuclide, RS is the radionuclide bound to sites S of the solid particles and X is a competitive element that can be replaced by R on sites S. k_1 and k_2 are the kinetic transfer coefficients, or absorption and desorption velocities, respectively.

The behaviour of Pu in the marine environment is especially complex since it can exist in different oxidation states simultaneously. Thus, Pu(III) and Pu(IV) predominate as the reduced and Pu(V) and Pu(VI) as the oxidized forms. The reduced Pu is highly particle-reactive and has been shown to possess a distribution coefficient that is two orders of magnitude higher than that of the more soluble oxidized Pu (McKay & Pattenden, 1993). Thus, the model described in Periáñez (2000b) was developed to simulate the dispersion of Pu in the eastern Irish Sea (where it is released from the Sellafield nuclear fuel reprocessing plant) under tidal dynamics and including redox reactions. The model solves simultaneously the hydrodynamic equations, the suspended matter equation and six equations whose solutions give the time evolution of reduced and oxidized Pu in the three phases considered (water, suspended matter and active bottom sediments, that consist of particles with diameter <62.5 μm). Redox reactions are described in terms of reaction velocities, which were deduced from the laboratory experiments of Boust et al. (1996). The kinetic transfer coefficients for the one-step model are considered to have different values for reduced and oxidized Pu. The model gave acceptable agreements between observed and computed Pu distributions in water, suspended matter and bottom sediments. Also, it allowed the computation of distribution coefficients for total, reduced and oxidized Pu. Although the model reproduced the observed percentage of oxidized Pu in water, it predicted that most Pu in the sediment was in an oxidized form, while it is known that it is present in a reduced form.

Recently, there has been evidence of re-dissolution of radionuclides from the contaminated sediments of the Irish Sea, which are now acting as a source of long-lived Sellafield waste radionuclides (Cook, MacKenzie, McDonald, & Jones, 1997; MacKenzie, Cook, McDonald, & Jones, 1998; Mitchell, Condren, León-Vintró, & McMahon, 1999). When the model was applied to simulate this re-dissolution from the sediments, estimated halving times were too low. Indeed, Cook et al. (1997) estimated a halving time of the order of 350 years for Pu concentrations in the sediment via the re-dissolution mechanism. On the other hand, model calculations

gave a halving time of 1.8 years. Very recent experiments (Ciffroy, Garnier, & Pham, 2001; El Mrabet, Abril, Manjón, & García-Tenorio, 2001) have shown that a model involving the existence of two successive reversible reactions properly simulates both the sorption and release kinetics. Thus, the model presented in Periáñez (2000b) has been refined using a two successive-step reversible model for the exchanges of radionuclides between the dissolved and solid phases. The objectives of this further development are:

- to develop a model that can be properly used to describe both the contamination of the sediment and the re-dissolution process when the sediment acts as a source of radionuclides to the water column. In particular, to obtain halving times in agreement with the value estimated from observations; and
- to improve the model results with respect to speciation of Pu between reduced and oxidized forms in the sediment.

It should be noted that this is the first time, to the author's knowledge, that a two-step kinetic model is implemented in a real full three-dimensional (3D) dispersion model.

2. The model

The exchange model that was used by Ciffroy et al. (2001) to describe their experiments considers two successive reversible reactions. The first describes a reversible isotopic or ion exchange process between dissolved radionuclides and some non-specific sites, S_1, present on the particle surfaces. The second slower reaction represents a reversible sorption to more specific sites, S_2. They can be represented as follows:

$$R + XS_1 \underset{k_2}{\overset{k_1}{\rightleftharpoons}} RS_1 + X \tag{2}$$

and

$$S_2 + RS_1 \underset{k_4}{\overset{k_3}{\rightleftharpoons}} RS_2 + S_1, \tag{3}$$

where k_3 and k_4 are the kinetic transfer coefficients, or sorption and release velocities, respectively, for the second reaction. The interaction between the dissolved and solid phases is described in the scheme of Fig. 1. The sorption of radionuclides is governed by kinetic coefficients k_1^{ox} and k_1^{red} for oxidized and reduced Pu, respectively. The release is governed by the same transfer coefficient k_2 for both oxidized and reduced forms, as described in Periáñez (2000b). The slower reaction that exchanges radionuclides between the non-specific and the specific sites is governed by the kinetic coefficients k_3 and k_4. As a first approximation, it is considered that these coefficients are the same for both the reduced and oxidized forms. Finally, redox reactions are governed by β_1 and β_2, which are the oxidation and reduction velocities, respectively. In the earlier version of the model, it was considered that these reaction velocities were the same in the three phases (water, suspended matter and bottom sediments).

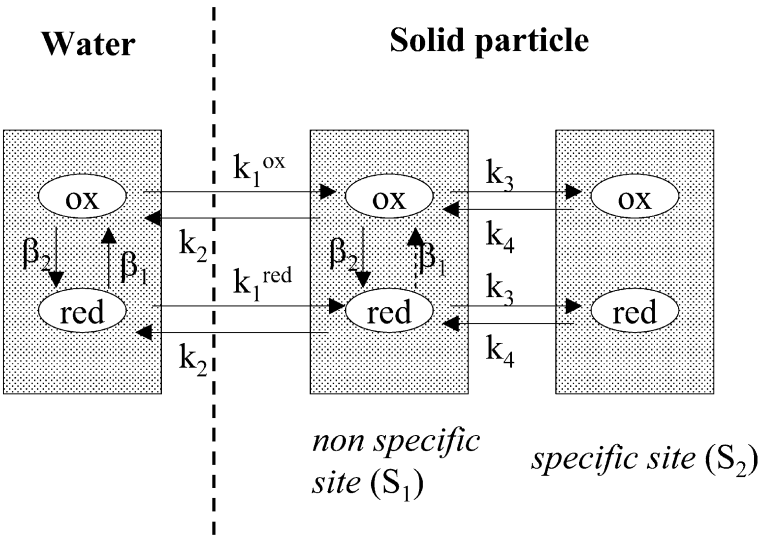

Fig. 1. Scheme showing the interaction between the liquid and solid phases. The oxidation reaction is considered in suspended matter, but it is not in the case of bottom sediments (dashed arrow). k_1 will be k_{11} if the solid particle is a suspended matter particle and k_{12} if it is a bottom sediment particle [see Eq. (4)].

As will be seen, model results are improved if the oxidation reaction is not considered in the bottom sediment (dashed arrow in Fig. 1) since there is experimental evidence supporting the fact that more than 90% of Pu in solid particles is in a reduced form (Mitchell et al., 1995). Of course, the oxidation reaction may exist in the sediment, but with a much smaller velocity than in the dissolved phase. Reaction velocities in the sediment have not been measured, thus it has been decided to remove such oxidation reaction since good results are obtained in this case. As in El Mrabet et al. (2001), it is assumed that the oxidation state does not change once Pu has reached the specific sites in solid particles.

The model solves the full 3D hydrodynamic equations using depth-following σ coordinates in the vertical with an appropriate set of boundary conditions. A flow-dependent eddy viscosity has also been used in the model. The 3D suspended matter equation is also solved simultaneously with the hydrodynamic equations. It includes advection–diffusion of particles, vertical fall (settling) and the input of suspended matter from the run-off of continental waters along the coastline. Deposition and erosion of the sediment are also incorporated into the sea-bed boundary condition of the equation. Equations are solved using finite difference schemes. Details can be seen in Periáñez (2000b) and will not be repeated here.

It is known that the sorption of dissolved radionuclides depends on the surface of particles per water volume unit. This quantity has been denoted as the exchange surface (Periáñez, 2000a, 2000b; Periáñez et al., 1996; Periáñez & Martínez-Aguirre, 1997). Thus,

$$k_1 = \chi_1(S_m + S_s) = k_{11} + k_{12}, \quad (4)$$

where S_m and S_s are the exchange surfaces for suspended matter and bottom sediments, respectively, and χ_1 is a parameter with the dimensions of a velocity denoted as the exchange velocity (Periáñez et al., 1996), which will have different values for the oxidized and reduced Pu. The exchange surfaces are easily obtained assuming spherical particles and a step function for the grain size distribution of particles (Periáñez et al., 1996):

$$S_m = \frac{3m}{\rho R} \tag{5}$$

and

$$S_s = \frac{3Lf\phi}{RH\Delta\sigma}, \tag{6}$$

where ρ is the suspended particle density, R is the mean radius of suspended matter and active sediment particles, m is the suspended matter concentration, H is water depth, $\Delta\sigma$ is the grid size in the vertical direction, L is the average mixing depth (the distance to which the dissolved phase penetrates the sediment), f gives the fraction of active sediment and ϕ is a correction factor that takes into account that not all of the sediment particle surface is in contact with water because some surface will be partially hidden by other sediment particles.

The modification to the equations presented in Periáñez (2000b) is the inclusion of the slow reaction to the equations that give the time evolution of activity concentrations in the solid phases. Thus, four new equations [Eqs. (11), (12), (15) and (16) in Appendix A] must also be added to the model, that give the time evolution of activity concentrations in the specific sites of suspended matter and bottom sediments and for both oxidized and reduced forms. A summary of the equations is presented in Appendix A.

3. Model results

The parameters used in the model are, of course, the same that were applied in Periáñez (2000b). Thus, the oxidation and reduction velocities are $\beta_1 = 1.85 \times 10^{-6}\ s^{-1}$ and $\beta_2 = 4.48 \times 10^{-7}\ s^{-1}$, respectively. The exchange velocities for the reduced and oxidized Pu are $\chi_1^{red} = 1.51 \times 10^{-4}\ m/s$ and $\chi_1^{ox} = 1.51 \times 10^{-6}\ m/s$, and the transfercoefficient k_2 is fixed as $1.16 \times 10^{-5}\ s^{-1}$ for both the reduced and oxidized forms. The new parameters introduced in the model are the kinetic coefficients controlling the slow reaction to the specific sites, k_3 and k_4. From the experiments of Ciffroy et al. (2001), it is obtained that k_3 is about one order of magnitude larger than k_4. On the other hand, El Mrabet et al. (2001) have measured a value of $1.4 \times 10^{-7}\ s^{-1}$ for k_3 in their experiments carried out with sea water from the southwest of Spain. Thus the following values were used in the model, since acceptable results were obtained with them:

$$k_3 = 1.2 \times 10^{-7}\ s^{-1}$$

and

$$k_4 = 1.2 \times 10^{-8}\ \mathrm{s}^{-1}.$$

Of course, model results could be refined if specific values for the Irish Sea are used when available.

The horizontal resolution of the model is $\Delta x = \Delta y = 5000$ m, 10 layers are used in the vertical (thus $\Delta\sigma = 0.1$) and the time step is fixed as $\Delta t = 60$ s. Water depths, presented in Fig. 2, were introduced from bathymetric maps.

Exactly the same simulations as those presented in Periáñez (2000b) were repeated with the new version of the model. Observed and computed distributions of ^{239,240}Pu have been compared for two years. The input from Sellafield was introduced in the model for each year. However, the input has been taking place since the 1950s. Thus, instead of starting the model from zero concentrations, we have assumed a uniform background in water, suspended matter and bottom sediments that represent the effect of previous discharges. It has been shown (Periáñez, Abril, & García-León, 1994) that model results do not depend upon the way the background is cre-

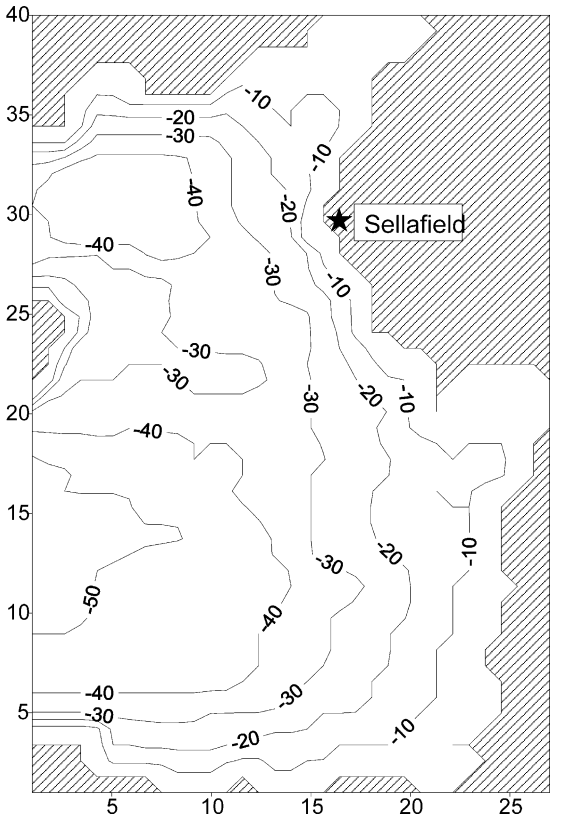

Fig. 2. Water depths (m) in the model domain. The star is Sellafield nuclear fuel reprocessing plant. Each unit in the *x* and *y* axis is 5000 m (grid cell number).

ated. Thus, the same results would be obtained if a large discharge is performed and some time is allowed to elapse so that the discharge is distributed over the sea. To save CPU time, the uniform background option was chosen. The background magnitude has been selected from a trial and error exercise: 0.01 Bq/g for suspended matter, 0.1 Bq/g for bottom sediments and 0.05 Bq/m^3 for water. Discharges from Sellafield are carried out over this background and model results are obtained after a simulation time of three months. These results are compared with observations (Periáñez, 2000b).

The computed distribution of total Pu in surface water for the year 1974 is presented in Fig. 3, together with the computed percentage of oxidized Pu as well as the observed Pu distribution (from Hetherington, 1976). If these maps are compared with those presented in Periáñez (2000b), it can be seen that model results are virtually the same as those obtained when the second slower reaction was not included. Activity levels over the sea are, in general, well reproduced by the model. Most Pu in solution is in an oxidized form. A higher content of reduced Pu only occurs close to the discharge point, due to the nature of the discharges. Indeed, Pu is released in a reduced form. An oxidation reaction then occurs causing over 90% of the Pu to be in an oxidized form (Mitchell et al., 1995). Our results are in agreement with these observations.

The computed distribution of total Pu in bottom sediments for the year 1977 is presented in Fig. 4. Again, this distribution is essentially the same as that obtained with the earlier version of the model. The important point is that, with the older model version, the maximum percentage of reduced Pu in the sediment was around 30% while now it is about 95%, in closer agreement with observations (McKay & Pattenden, 1993).

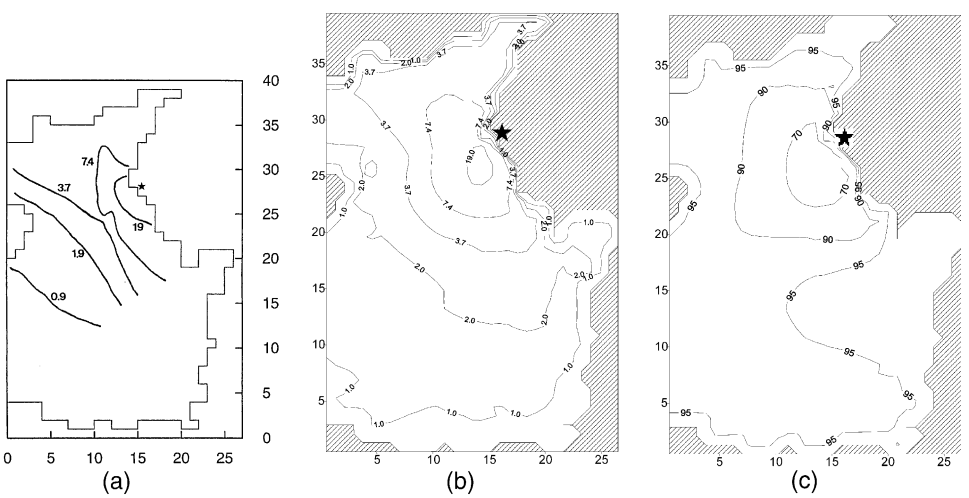

Fig. 3. Distribution of Pu (Bq/m^3) in surface water for the year 1974: (a) measured (Hetherington, 1976), (b) computed and (c) computed percentage of oxidized Pu. Each unit in the *x* and *y* axis is 5000 m (grid cell number).

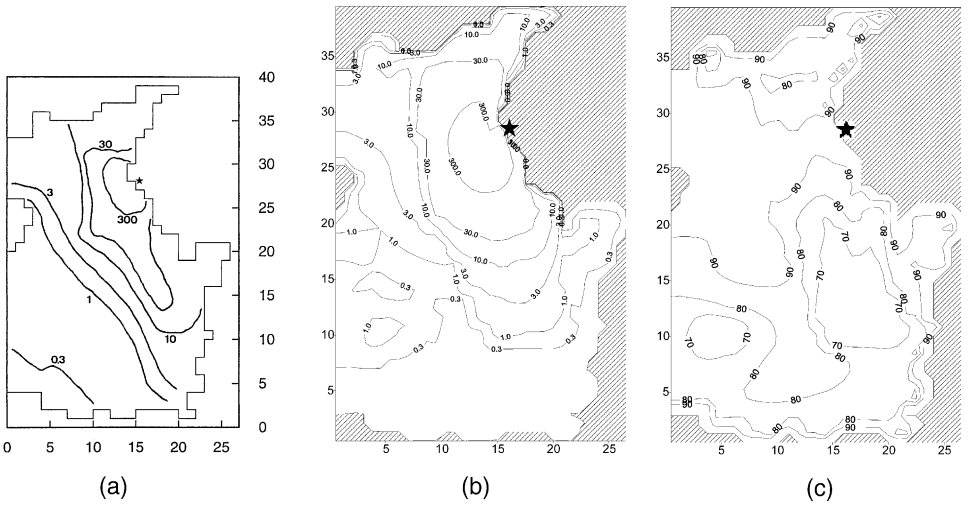

Fig. 4. Distribution of Pu (kBq/m²) in bottom sediments for the year 1977: (a) measured (Pentreath, 1985), (b) computed and (c) computed percentage of reduced Pu. Each unit in the *x* and *y* axis is 5000 m (grid cell number).

The model has also been used to simulate the re-dissolution process from the contaminated sediments. The model was started from actual concentrations in sediments and no input from Sellafield was introduced. Zero concentrations were also assumed for water and suspended matter. The time evolution of total Pu (reduced plus oxidized) in water and active sediment at a point close to Sellafield outlet are shown in Fig. 5 ("model" line). It can be seen that Pu concentrations in water increase due to redissolution from the contaminated sediment. Obviously, Pu content in the sediment decreases simultaneously. Oscillations at the same frequency as tidal oscillations are also apparent in water.

It can be seen in Fig. 5(b) that, in one month, Pu concentration in the sediment decreases by approximately 10^{-2} Bq/g. Considering an average sediment bulk density of $\rho_m = 900\ \mathrm{kg/m^{-3}}$, an average mixing depth $L = 0.1$ m and an average fraction of active sediment $f = 0.5$, the mass of active sediment in one grid cell is

$$\Delta x \Delta y L \rho_m f = 1.125 \times 10^9 \text{ kg}.$$

Thus, approximately 1.125×10^{10} Bq are introduced into the water column from the sediment in one month and in one cell. Assuming that the re-dissolution rate is constant and that the number of cells that are mainly contributing to the re-dissolution process is of the order of 20 (those located around Sellafield, which have the most contaminated sediments), it results that some 2.7×10^{12} Bq of Pu are annually incorporated to the sea water from the sediment. This number, although a rough estimation, can be compared with the value obtained by Cook et al. (1997) from observations: 1.2×10^{12} Bq.

Two maps showing the computed Pu distribution in water and the computed distribution coefficient, k_d, for total Pu 30 days after the beginning of the experiment are

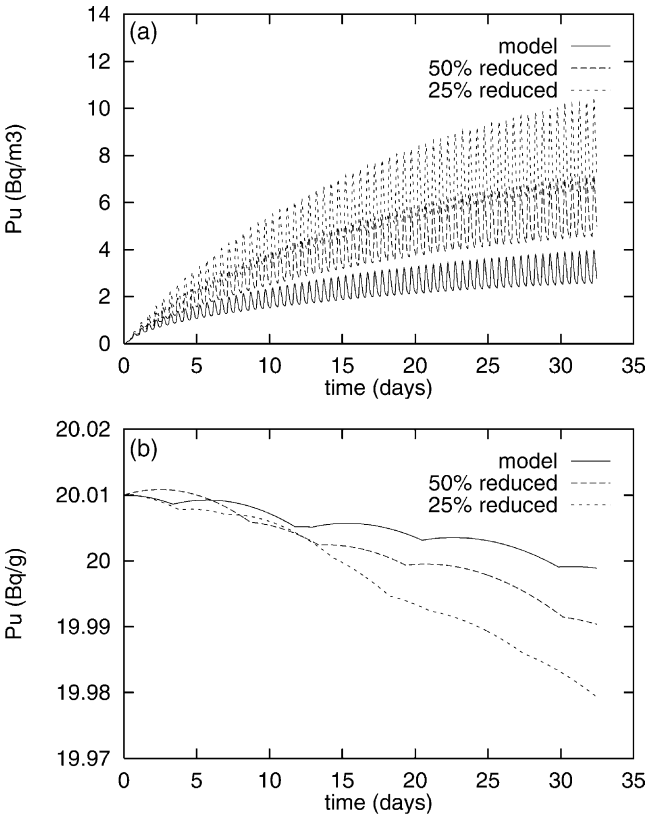

Fig. 5. Time evolution of Pu concentrations, (a) in water and (b) in active sediment, in Bq/m^3 and Bq/g, respectively, for different values of the initial percentage of reduced Pu in the sediment; 50% and 25% reduced mean that only such percentage of the Pu content in the sediment is initially considered to be in a reduced form over the model domain. The "model" line corresponds to the simulation started from the real distribution of Pu between the oxidized an reduced forms [presented in Fig. 4(c)].

presented in Fig. 6. The Pu distribution in water produced by the re-dissolution process is similar to that due to the direct discharges from Sellafield [compare Figs. 3(b) and 6(a)]. However, the distribution of the k_d is clearly different. When Sellafield discharges are carried out, k_ds of the order of 10^5 l/kg are obtained over the sea (Periáñez, 2000b), in agreement with the observations of Mitchell et al. (1995) and with the value recommended by IAEA (1985). The model simulations also predict that k_ds diminish with increasing distance from Sellafield. This effect, also observed (Mitchell et al., 1995), was attributed to the nature of the discharges since almost all Pu in the releases is associated with suspended particles. On the other hand, k_ds of the order of 10^4 l/kg are obtained from the model re-dissolution experiment, smaller than the equilibrium value (IAEA, 1985). Moreover, now model results do not present a decrease in the k_d with increasing distance from Sellafield.

It is possible to compute the sediment halving time by numerical fitting of the

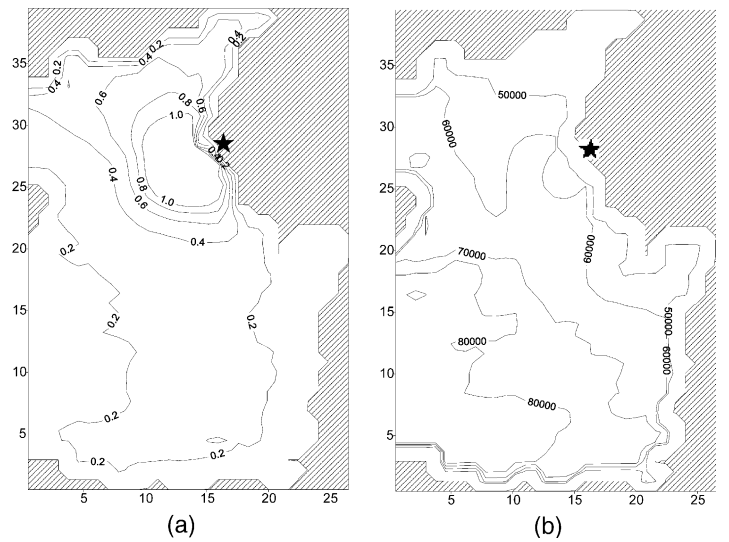

Fig. 6. Computed distribution maps of (a) total Pu in water (Bq/m^3) and (b) total Pu k_d (l/kg) in the re-dissolution experiment. Each unit in the x and y axis is 5000 m (grid cell number).

time evolution of the total Pu content in the sediment to an exponential decay function. The sediment halving time obtained in this way is 112 years, in agreement (by order of magnitude) with the estimation from observations carried out by Cook et al. (1997), 350 years. This is clearly in contrast with the halving time of 1.8 years computed with the earlier version of the model. However, model results could probably be improved if k_3 and k_4 specific values for the eastern Irish Sea were used. Thus, it seems that it is necessary to consider two consecutive reversible reactions to properly simulate re-dissolution from a contaminated sediment. The oxidation state of Pu in the sediment also affects the halving time. If only 50% of Pu in the sediment is considered to be in a reduced form, then the halving time reduces to 60 years. A reduction to 39 years is obtained if only 25% of Pu is considered to be initially reduced in the sediment. Indeed, it can be seen in Fig. 5 how Pu concentrations in the sediment decrease faster as the percentage of reduced Pu in the sediment decreases.

4. Conclusions

The model presented in Periáñez (2000b) has been refined removing the oxidation reaction in bottom sediments and considering a two-step kinetics to describe the interactions between the dissolved and solid phases consisting of two consecutive reversible reactions.

From our calculations, it is concluded that a one-step kinetic model is enough to properly simulate the contamination of sediments due to a external input of radionuclides since results obtained with the one-step and the two-step models are essentially the same. Such one-step models have been widely used before (Aldridge, 1998;

Margvelashvily et al., 1997; Periáñez, 2000a, 2000b; Periáñez et al., 1996; Piasecki, 1998). However, if the interest consists of studying the re-dissolution of radionuclides from a contaminated sediment and subsequent transport, it seems clear that a two-step model must be applied. A halving time computed with the one-step model is two orders of magnitude lower than the value estimated from observations, while halving time computed with the two-step model is of the same order of magnitude as field observations. On the other hand, it has been pointed out that the oxidation state of Pu in the sediment affects the re-dissolution process, in such a way that halving time can be significantly reduced if most Pu in the sediment is in an oxidized form. Finally, the removal of the oxidation reaction in the sediment leads to a more realistic distribution of Pu between the reduced and oxidized forms in the sediment.

Acknowledgements

This work was supported by ENRESA and the EU 5th Framework Programme (1998–2002) Nuclear Fission and Radiation Protection, Contract FIGE-CT-2000-00085.

Appendix A

A.1. Solution

The equation that gives the temporal evolution of oxidized Pu in solution, C_d^{ox} (Bq/m^3), is:

$$\frac{\partial C_d^{ox}}{\partial t} = (\text{adv} + \text{dif})_{3D} - (k_{11}^{ox} + \pi k_{12}^{ox}) C_d^{ox} + k_2 \left(m C_s^{ox} + \pi \frac{A_s^{ox} L \rho_m f \phi}{H \Delta \sigma} \times 10^{-3} \right) - \lambda C_d^{ox} + \beta_1 C_d^{red} - \beta_2 C_d^{ox}, \quad (7)$$

where $(\text{adv+dif})_{3D}$ represents three-dimensional advection and diffusion of radionuclides. $\pi = 0$ unless we are solving the equation for the water layer that is in contact with the sediment; in this case $\pi = 1$ to allow the transfer of radionuclides between the water and the bottom sediment. C_s^{ox} and A_s^{ox} (both in Bq/g) are oxidized Pu concentrations in suspended matter and active sediment respectively. The sediment bulk density, ρ_m, is given in kg/m^3 and λ is the radioactive decay constant. The external source of radionuclides must be added to this equation in the points where it exists.

A similar equation is deduced for reduced Pu in solution, C_d^{red}:

$$\frac{\partial C_d^{red}}{\partial t} = (\text{adv} + \text{dif})_{3D} - (k_{11}^{red} + \pi k_{12}^{red}) C_d^{red} + k_2 \quad (8)$$

$$\left(mC_s^{red} + \pi\frac{A_s^{red}L\rho_m f\phi}{H\Delta\sigma}\times 10^{-3}\right) - \lambda C_d^{red} - \beta_1 C_d^{red} + \beta_2 C_d^{ox},$$

with obvious meanings for the notation.

A.2. Suspended matter

For the oxidized Pu:

$$\frac{\partial(mC_s^{ox})}{\partial t} = (\text{adv} + \text{dif})_{3D} - \text{sett}^{ox} + \pi(\text{res} - \text{dep})^{ox} + k_{11}^{ox}C_d^{ox} - k_2 mC_s^{ox} \qquad (9)$$
$$-\lambda mC_s^{ox} + m(\beta_1 C_s^{red} - \beta_2 C_s^{ox} - k_3 C_s^{ox} + k_4^* C_s^{ox}),$$

where sett, res and dep means settling, resuspension and deposition of particles (Periáñez, 2000b). Note that the last terms in this equation represent the second reaction; that is, the exchange of radionuclides with the specific sites. Radionuclide concentrations and processes associated with the specific sites are denoted by an asterisk at the left. The equation for the reduced Pu is:

$$\frac{\partial(mC_s^{red})}{\partial t} = (\text{adv} + \text{dif})_{3D} - \text{sett}^{red} + \pi(\text{res} - \text{dep})^{red} + k_{11}^{red}C_d^{red} - k_2 mC_s^{red} \qquad (10)$$
$$-\lambda mC_s^{red} + m(-\beta_1 C_s^{red} + \beta_2 C_s^{ox} - k_3 C_s^{red} + k_4^* C_s^{red}).$$

The equations that give the time evolution of concentrations in the specific sites are:

$$\frac{\partial(m^*C_s^{ox})}{\partial t} = {}^*(\text{adv} + \text{dif})_{3D} - {}^*\text{sett}^{ox} + \pi^*(\text{res} - \text{dep})^{ox} - \lambda m^* C_s^{ox} \qquad (11)$$
$$+ m(k_3 C_s^{ox} - k_4^* C_s^{ox})$$

and

$$\frac{\partial(m^*C_s^{red})}{\partial t} = {}^*(\text{adv} + \text{dif})_{3D} - {}^*\text{sett}^{red} + \pi^*(\text{res} - \text{dep})^{red} - \lambda m\ {}^*C_s^{red} \qquad (12)$$
$$+ m(k_3 C_s^{red} - k_4^* C_s^{red}).$$

A.3. Active sediments

Oxidized Pu:

$$\frac{\partial A_s^{ox}}{\partial t} = k_{12}^{ox}\frac{C_d^{ox}(b)H\Delta\sigma}{L\rho_s f}\times 10^{-3} - k_2\phi A_s^{ox} + (\text{dep} - \text{res})^{ox} - \lambda A_s^{ox} - \beta_2 A_s^{ox} \qquad (13)$$
$$-k_3 A_s^{ox} + k_4^* A_s^{ox},$$

where (b) means that this parameter must be evaluated at the deepest water layer (in contact with the sediment).

In the case of reduced Pu:

$$\frac{\partial A_s^{red}}{\partial t} = k_{12}^{red}\frac{C_d^{red}(b)H\Delta\sigma}{L\rho_s f} \times 10^{-3} - k_2\phi A_s^{red} + (\text{dep}-\text{res})^{red} - \lambda A_s^{red} + \beta_2 A_s^{ox} \quad (14)$$
$$- k_3 A_s^{red} + k_4^* A_s^{red}.$$

Specific sites:

$$\frac{\partial^* A_s^{ox}}{\partial t} = {}^*(\text{dep}-\text{res})^{ox} - \lambda^* A_s^{ox} + k_3 A_s^{ox} - k_4^* A_s^{ox} \quad (15)$$

and

$$\frac{\partial^* A_s^{red}}{\partial t} = {}^*(\text{dep}-\text{res})^{red} - \lambda^* A_s^{red} + k_3 A_s^{red} - k_4^* A_s^{red}. \quad (16)$$

References

Aldridge, J. N. (1998). A model for prediction of marine radionuclide transport in both particulate and dissolved phases. *Radiation Protection Dosimetry*, *75*, 99–103.

Boust, D., Mitchell, P. I., Garcia, K., Condren, O. M., León-Vintró, L., & Leclerc, G. (1996). A comparative study of the sepciation and behaviour of plutonium in the marine environment of two reprocessing plants. *Radiochimica Acta*, *74*, 203–210.

Ciffroy, P., Garnier, J. M., & Pham, M. K. (2001). Kinetics of the adsorption and desorption of radionuclides of Co, Mn, Cs, Fe, Ag and Cd in freshwater systems: experimental and modelling approaches. *Journal of Environmental Radioactivity*, *55*, 71–91.

Cook, G. T., MacKenzie, A. B., McDonald, P., & Jones, S. R. (1997). Remobilization of Sellafield derived radionuclides and transport from the north east Irish Sea. *Journal of Environmental Radioactivity*, *35*, 227–241.

El Mrabet, R., Abril, J. M., Manjón, G., & García-Tenorio, R. (2001). Experimental and modelling study of plutonium uptake by suspended matter in aquatic environments from southern Spain. *Water Research*, *35*, 4184–4190.

Hetherington, J. A. (1976). The behaviour of plutonium in the Irish Sea. In M. N. Miller, & J. N. Stannar (Eds.), *Environmental toxicity of aquatic radionuclides. Models and mechanisms* (pp. 81–106). Ann Arbor: Ann Arbor Science Publishers.

IAEA (1985). *Sediment k_d and concentration factors for radionuclides in the marine environment*. Technical Report Series 247. Vienna: IAEA.

MacKenzie, A. B., Cook, G. T., McDonald, P., & Jones, S. R. (1998). The influence of mixing timescales and re-dissolution processes on the distribution of radionuclides in the northeast Irish Sea sediments. *Journal of Environmental Radioactivity*, *39*, 35–53.

Margvelashvily, N., Maderich, V., & Zheleznyak, M. (1997). Threetox: a computer code to simulate three dimensional dispersion of radionuclides in stratified water bodies. *Radiation Protection Dosimetry*, *73*, 177–180.

McKay, W. A., & Pattenden, N. J. (1993). The behaviour of plutonium and americium in the shoreline waters of the Irish Sea: a review of Harwell studies in the 1980s. *Journal of Environmental Radioactivity*, *18*, 99–132.

Mitchell, P. I., Condren, O. M., León-Vintró, L., & McMahon, C. A. (1999). Trends in plutonium, americium and radiocaesium accumulation and long-term bioavailability in the western Irish Sea mud basin. *Journal of Environmental Radioactivity*, *44*, 223–251.

Mitchell, P. I., Vives i Batlle, J., Downes, A. B., Condren, O. M., León-Vintró, L., & Sánchez-Cabeza,

J. A. (1995). Recent observations on the physico-chemical speciation of plutonium in the Irish Sea and the western Mediterranean. *Applied Radiation Isotopes, 46*, 1175–1190.

Pentreath, R. J. (1985). *Behaviour of radionuclides released into coastal waters*. IAEA TECDOC 329. Vienna: IAEA.

Periáñez, R. (2000a). Modelling the tidal dispersion of ^{137}Cs and ^{239,240}Pu in the English Channel. *Journal of Environmental Radioactivity, 49*, 259–277.

Periáñez, R. (2000b). Modelling the physico-chemical speciation of plutonium in the eastern Irish Sea. *Journal of Environmental Radioactivity, 49*, 11–33.

Periáñez, R., Abril, J. M., & García-León, M. (1994). A modelling study of ^{226}Ra dispersion in an estuarine system in southwest Spain. *Journal of Environmental Radioactivity, 24*, 159–179.

Periáñez, R., Abril, J. M., & García-León, M. (1996). Modelling the dispersion of non conservative radionuclides in tidal waters. Part 1: conceptual and mathematical model. *Journal of Environmental Radioactivity, 31*, 127–141.

Periáñez, R., & Martínez-Aguirre, A. (1997). U and Th concentrations in an estuary affected by phosphate fertilizer processing: experimental results and a modelling study. *Journal of Environmental Radioactivity, 35*, 281–304.

Piasecki, M. (1998). Transport of radionuclides incorporating cohesive/non cohesive sediments. *Journal of Marine Environmental Engineering, 4*, 331–365.